Aging of hemp shiv used for concrete

Guillaume Delannoy, Sandrine Marceau, Philippe Gle, Etienne Gourlay, Marielle Gueguen Minerbe, Dinarzed Diafi, Issam Nour, Sofiane Amziane, Fabienne Farcas

AGING OF HEMP SHIV USED FOR CONCRETE

Guillaume Delannoy[a], Sandrine Marceau[a*], Philippe Glé[bc], Etienne Gourlay[b], Marielle Gueguen-Minerbe[a], Dinarzed Diafi[a], Issam Nour[a], Sofiane Amziane[d], Fabienne Farcas[a]

[a] Paris-Est University, MAST/CPDM/IFSTTAR 77447 Marne-la-Vallée Cedex 2, France; guillaume.delannoy@ifsttar.fr; sandrine.marceau@ifsttar.fr; marielle-gueguen@ifsttar.fr; dinarzed.diafi@ifsttar.fr; issam.nour@ifsttar.fr; fabienne.farcas@ifsttar.fr

[b] CEREMA, Laboratory of Strasbourg, 11 rue Jean Mentelin, BP 9, 67035 Strasbourg Cedex 2, France;
philippe.gle@cerema.fr; etienne.gourlay@ifsttar.fr

[c] CEREMA, IFSTTAR, UMRAE, 11 rue Jean Mentelin, BP 9, 67035 Strasbourg Cedex 2, France;

[d] University of Clermont Auvergne, Institut Pascal, UMR 6602, 63174 Aubière Cedex, France.
sofiane.amziane@uca.fr

Corresponding author: sandrine.marceau@ifsttar.fr

Abstract

Functional properties of vegetal concretes, such as hygrothermal and acoustical properties, are brought by the microstructure of the vegetal particles. However, data are necessary to develop biobased insulation materials by providing results on their long-term behaviour, and only few studies focus on this topic. A first step is to characterize the behaviour of vegetal aggregates in bulk.

In this study, hemp shiv is stored for two years in three different conditions: a static environment used as reference, accelerated aging conditions based on humidification and drying cycles, and an exterior aging. The potential evolution of functional properties of particles is monitored with time and depending on the aging conditions. These evolutions are understood thanks to a study at a microscopic scale, where the microstructure of the particles is investigated.

This study shows that no variation is observed for the reference conditions, whereas four phenomena linked to aging can be identified for accelerated and exterior aging conditions: a mass loss, volume variations of the particles and an opening of the aggregates porosity for

both storing conditions. The last one, only observed for exterior aging, is a modification of the pore size distributions.

Keywords

Vegetal aggregate; hemp shiv; hygrothermal and acoustical properties; microstructure; microorganisms.

1 INTRODUCTION

The advent of biobased materials has come about in response to a desire to use products with low environmental impact, made from renewable raw materials. In the building sector, biobased construction materials are in use, such as wood for structural frameworks or biobased insulation materials. Biobased insulators, and notably plant-based concretes, are being used increasingly frequently due to their thermal, hygrothermal and acoustic performances [1]. These functional properties are the result of the vegetal aggregates employed in the formulation [2], whilst mechanical strength is provided by the presence of frame. Numerous studies have been carried out on defining and understanding the properties of the material, or optimising the formulations used. A number of recent studies have looked at the durability and long-term behaviour of these insulators [3], [4], [5], [6], [7], but the accelerated aging processes are much too short or overly severe in comparison to real-world conditions of use, such as the application of freeze–thaw cycles [3]. However, lack of knowledge about the evolution of the properties of plant-based concretes over time is a barrier to the development of these materials. Indeed, the lack of guarantee as to the durability of the desired properties over a given period of time does not inspire confidence in users, architects or insurance companies.

It is for these reasons that a study is conducted on the durability of hemp-based concretes, with the aim of identifying the mechanisms which cause the functional properties of the material to change. However, to date, there has been no study done of the change over time observed in the plant aggregates on their own, although it is these particles which are responsible for a large proportion of the properties for which the material is used. In order to understand the mechanisms of aging of plant-based concretes, it seems essential to understand the behaviour of the particles in bulk over time. With a similar chemical composition, made up of cellulose, hemicellulose and lignins for the most part, it is possible to draw inspiration from the numerous studies examining the durability of wood.

Durability studies on wood have produced standards which guarantee quality and users' expectations over a given period of time, in set usage conditions and with an amount of maintenance [8]. Depending on the application, specific wood species are chosen according to the applications and the conditions of use. Most of the published work concerns solid wood [9] [10] [11] [12] [13] [14] [15] [16], but some of them are dedicated to wood pellets [17] [18]. Aging conditions correspond to outdoors environments [9] [10] [17] [14] [15] [16] or

are accelerated in laboratory [11] [18] [12] [13]. Various aging factors are applied on wood in these studies, such as immersion in water for periods from 10 days at 60 and 90°C [11] to 8 and 2000 years in natural conditions [9] [10], variations of relative humidity during 20 days [12] to one year [18] [17], exposure to UV aging until four weeks [13] or natural aging without protection during several years [14] [17]. Therefore, depending on the study in question, the aging conditions are very different in terms of environment or exposure duration. Whatever the protocols used, the functional properties are monitored over time, namely mostly mechanical and/or hygroscopic properties [17], [18] [19] [15] [16], but also acoustic properties [20]. Overall, aging leads to deterioration in the mechanical properties and to an increase in water sorption capacity. Other parameters which characterise the microstructure of the material are also studied, such as porosity, swelling, or variations in weight of the materials. The variations of functional and microstructural properties are often explained by a change in the chemical compositions of the wood, usually due to the degradation of the lignin or hemicellulose [21]. These chemical degradations may result from photo-oxidation or thermo-oxidation reactions, but above all, from the action of micro-organisms which can grow on lignocellulosic materials in high humidity conditions. Indeed, the micro-organisms use the cellulosic materials as a nutrient [22], and they may, selectively or otherwise, attack pectin, lignins, hemicellulose or cellulose. These micro-organisms are present in the air and in water, but also in the plants as they grow. Indeed, in order to separate the fibres from the stalks more easily, the material may be retted for a time, enabling the micro-organisms to consume the pectin which binds the fibres together. Therefore, such retting impacts upon the properties of the materials [23]. There are various tests of resistance to the growth of micro-organisms, placing the plant materials inoculated with moulds in conditions of high hygrometry, as for example 26°C and 85 and 95% RH [24], or 20°C and 70% RH [25]. The result of an attack by micro-organisms is a loss of mass of the materials, which can lead to structural alterations which modify the functional properties, such as mechanical properties.

In view of these results, three environments are chosen in this study to assess the durability of hemp aggregates used for vegetal concretes. The first offers stable conditions and is used as a reference point. The second one is an accelerated aging imposing variations in humidity. The relative humidity varies from 40% RH to 98% at a fixed temperature of 30°C. Indeed, in the normal conditions of use of hemp concrete, unlike wood, hemp shiv should never be exposed to direct UV light or to liquid water. This temperature favours the development of micro-organisms, which has been identified as a significant degradation factor. Finally, a harsher, outdoor aging process is used.

The objective of this article is to identify the mechanism by which hemp shiv ages in the presence of moisture. The potential evolution of the functional properties of the material (acoustic and hydric properties) is characterised and linked to the microstructural changes (density, porosity, etc.) occurring in the different environments. The discussion focuses on understanding the mechanisms of aging of hemp shiv.

2 MATERIALS AND METHODS

2.1 Materials

A commercial hemp shiv, sold for an insulation application, is selected for this study. To analyse homogenous samples of particles, batches of 100 g are sampled from an entire 200 L bag of shiv as recommended by RILEM TC 236-BBM.

The initial rate of water absorption, the absorption coefficient, the granulometry (particle size distribution, PSD) and the quantity of fibres and dust are measured in accordance with the RILEM recommendations [26].

The quantity of soluble compounds is determined by the loss of mass of hemp shiv powder after 1 hour of immersion at 100°C. 4g of hemp powder are analysed, with a water/hemp ratio of 100. To obtain the powder, a batch of shiv is crushed and sieved at 500 µm. The results are presented in Table 1 and Figure 1.

	Initial rate of water absorption IRA (%)	Absorption coefficient K_1 (%/log(t))	Fibre and dust content (%)	Hot water soluble compounds (%)
Hemp shiv	IRA = 197 ± 6	K_1 = 50 ± 3	Fibre: 3.3 ± 0.6 Dust: 0.5 ± 0.2	11.8 ± 0.7

Table 1. Physical properties of hemp shiv

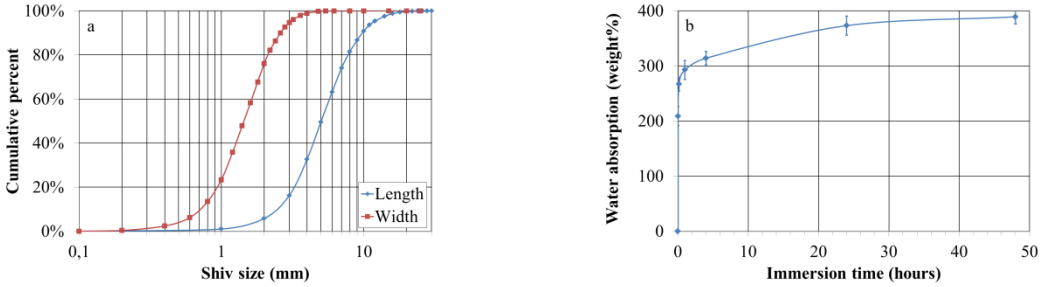

Figure 1. a) PSD of hemp shiv obtained by image analysis; b) Water absorption of hemp shiv

2.2 Aging protocols

The hemp particles are submitted to three different environments in this study.

The first is used as reference and correspond to static conditions, at 20°C and 50% RH. This is referred as A_{Ref}, and serves as a control for the potential evolution of the properties of hemp shiv even when no particular stress is applied.

The second is an accelerated aging process. The shiv is placed in a fine-meshed metal basket in an environmental chamber. At a constant temperature of 30°C, humidification and drying cycles are applied, with 5 days at 98% RH and 2 days at 40% RH. The choice of these

parameters is based on a previous study [6]. The transitions of relative humidity take place over the course of an hour. This aging protocol is denoted A_{HD}.

To observe more severe aging of the hemp shiv, a last batch is placed in the same kind of basket, outside (Figure 2), and subjected to various weather conditions, including sunlight, rain, snow and temperature variations. This last aging condition is denoted A_{Ext}.

Figure 2. Sample of hemp shiv aged during two years in A_{Ext} conditions

For A_{Ref} and A_{HD}, which are controlled conditions, different measurements are taken from 0 (A_0) to two years of aging. In the case of A_{Ext}, where nothing is controlled, fewer measurements are made during the two years.

2.3 Functional properties

The acoustic properties are measured using a Kundt tube (AcoustiTube AFD). Two types of properties are obtained: the acoustic absorption coefficient α and the transmission loss TL. The acoustic absorption coefficient is the proportion of sound energy absorbed by a material. It is expressed for values ranging between 1 (total absorption, no reflection) and 0 (no absorption, total reflection). The transmission loss (expressed in decibels) represents the sound insulation provided by a material. 3 measurements are taken for each batch of bulk shiv over a frequency range [250-2000Hz]. At A_0, the batches contain 40.7 g of hemp shiv, to obtain a controlled density of 130 $kg.m^{-3}$ in the volume of the sample chamber (10 cm in diameter and 4 cm in height). The different batches are aged and reused for the acoustic measurements.

The hydric behaviour is determined on the basis of the water vapour sorption isotherms using a DVS machine (Dynamic Vapour Sorption – SMS DVS Advantage). A few granules representing a few tens of mg are suspended in a microbalance within a sealed thermostatically controlled chamber at 25°C. The schedule for the DVS is set to start at 0% RH up to 95%. A given relative humidity is applied until the weight change of the sample is less than $0.0005\%.min^{-1}$ or during 12 hours if the weight is not stabilised. Sorption isotherms are produced by plotting mass change against relative humidity (RH) and illustrate the water vapour sorption capacity as a function of the relative humidity. The overall sorption behaviour across the whole range of relative humidity values is simulated using the GAB model, as described in an earlier study [2]. The specific surface of water vapour sorption S_m is deduced with this model.

2.4 Microstructure characterisation

Microstructure of hemp shiv is characterised by densities measurements, acoustic parameters and SEM observations.

For bulk shiv, three types of volume fractions can be identified [27], and are represented in Figure 3:

- the volume fraction constituted by the vegetal cell walls of the hemp shiv, noted as $\eta_{cell\ wall}$;
- the volume fraction of air between the particles, or interparticle porosity Φ_{inter}, which is due to an imperfect arrangement of the hemp shiv. These pores are around a millimetre in size;
- the volume fraction of air within the particles, or intraparticle porosity Φ_{intra}, with pore diameters generally ranging from 3-10 nm for mesopores, to 0.1-1 µm and 20-80 µm for macropores [28].

Depending on the kind of porosity, it may be open and accessible for measurement, open but not accessible to measurement, or closed. With a pore size in the millimetre range, the interparticle porosity, represented in grey in Figure 3, is always open and accessible. On the other hand, the intraparticle porosity may contain closed pores and pores not accessible to the measurement. For simplicity's sake, no distinction is drawn between intraparticle porosity which is closed or open but not accessible; both are denoted by Φ_{intra_closed}. This category is randomly represented in dark green in the diagram. The open and accessible intraparticle porosity (in light green) is called Φ_{intra_opened}.

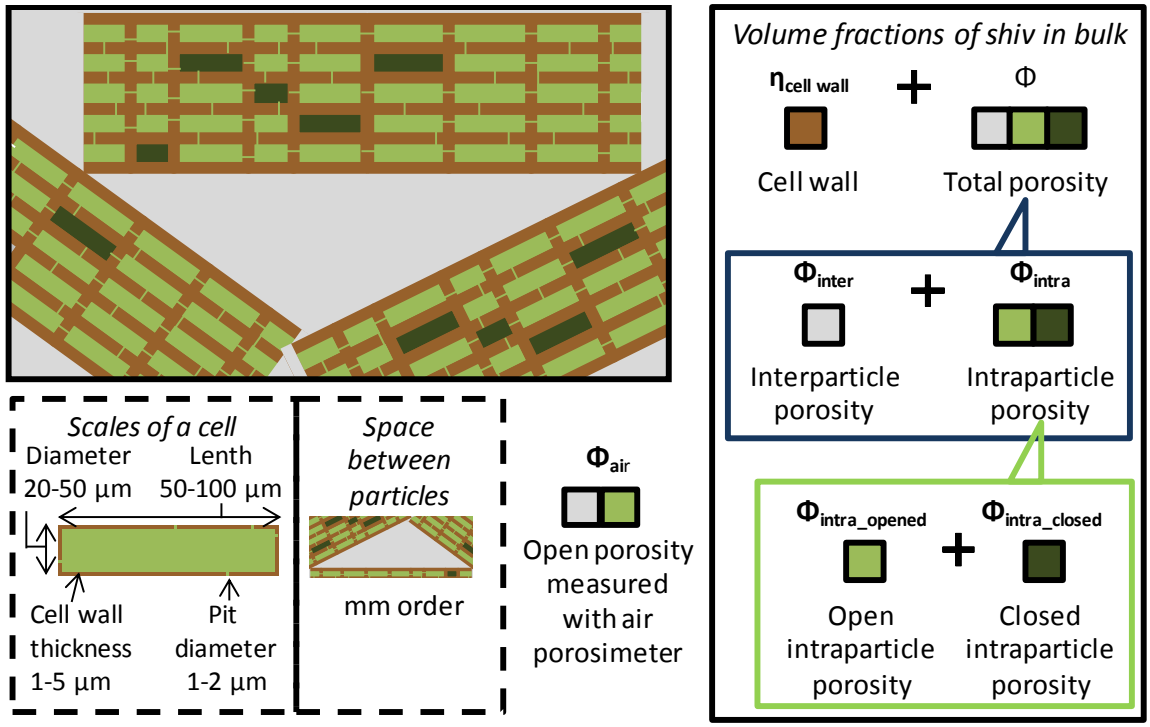

Figure 3. Representation of the different types of volume fractions for shiv in bulk, porosity open to the air and pore sizes

By combining different techniques, it is possible to quantify the different volume fractions corresponding to the vegetal part or to each type of porosity. In all cases, these volume fractions are expressed as a function of a volume of bulk shiv.

The bulk density ρ of the hemp shiv is the ratio of the mass of a batch of bulk hemp shiv to the volume it occupies in unstressed conditions. The RILEM protocol [26] is applied to around 100 g of particles to obtain this parameter.

The density of the plant cell wall $\rho_{cell\ wall}$ is an intrinsic value of the material, which depends on its chemical composition. In this case, the vegetal cell wall is expected not to contain any porosity. The volume corresponding to the vegetal cell walls of the material is measured by introducing a fluid into the pores in the material. Knowing the mass of the sample introduced, the density of the vegetal part can then be calculated. To measure this density, the hemp shiv is ground to a powder of grain size less than 500 µm in order to eliminate the porosities of the vegetal cell walls. The volume of the powder is then measured using a helium pycnometer (Micromeritics AccuPyc II 1340, volume 10 cm^3, pressure 19.5 psi, stability criterion 0.005 psi/min).

To come closer to real conditions of use of the materials, air porosity has also been determined on bulk hemp shiv as described by Gourlay [29]. In this case, as O_2 and N_2 molecules are larger than the helium atom, a portion of the pores is closed or inaccessible for

measurement. Accordingly, the evolution of the skeleton density ρ_{sk} during the material aging is monitored with this technique. A distinction must be drawn between the density of the cell wall $\rho_{cell\ wall}$, which does not contain any porosity, and the density of the skeleton ρ_{sk}, where closed or inaccessible pores are included into the volume of the vegetal skeleton.

The total porosity Φ, which is the combination of Φ_{inter} and Φ_{intra}, can be evaluated on the basis of the density of the plant cell wall and of the bulk density, using the following equation:

$$\Phi = 1 - \frac{\rho}{\rho_{cell\ wall}}$$

The volume fraction of solid material $\eta_{vegetal}$ is the remaining volume fraction:

$$\eta_{vegetal} = 1 - \Phi$$

The porosity accessible to air Φ_{air} is calculated using the value of the bulk density ρ and the skeleton density ρ_{sk}.

$$\Phi_{air} = 1 - \frac{\rho}{\rho_{sk}}$$

Based on acoustic measurements and using the model developed by Zwikker and Kosten [30], it is possible to calculate the acoustic porosity, which represents the porosity causing the dissipation of a soundwave in the material. As the acoustic properties mainly depend on the interparticle porosity [27], it is possible to estimate this porosity using the value of the acoustic porosity Φ_{acou} by assuming that it corresponds to Φ_{inter}.

When the interparticle porosity is known, it is possible to deduce the open intraparticle porosity Φ_{intra_opened} using the following equation:

$$\Phi_{intra\_opened} = \Phi_{air} - \Phi_{inter} \approx \Phi_{air} - \Phi_{acou}$$

Finally, Φ_{intra_closed} is calculated on the basis of the difference between the total porosity and the open porosity:

$$\Phi_{intra\_closed} = \Phi - \Phi_{air}$$

Other parameters describing the microstructure of the material are obtained from the acoustical measurements [27]:

- σ, the airflow resistance of the material;
- α_{∞}, the tortuosity describing the sinuosity of the porous network;
- Λ, the characteristic viscous length which corresponds to an estimation of the size of interconnection between pores.

The microstructure is also observed with a scanning electron microscope (SEM) FEI Quanta 400 in secondary electron mode on both longitudinal and transverse slices of hemp shiv.

2.5 Chemical analysis

The chemical composition of hemp shiv is determined by the Van Soest method, following the standard NF V18-122 [31]. Dry hemp shiv powder is added in a neutral detergent solution in order to extract all kind of molecules excepting cellulose, hemicellulose and lignin. A second immersion in an acid detergent solution extracts hemicellulose. After sulphuric acid treatment, cellulose is hydrolysed and extracted. By mass differences, proportions of cellulose, hemicellulose, lignin and the other compounds are deduced per mass of dry material.

3 RESULTS

3.1 Functional properties of shiv

First, the results of the monitoring of the functional properties over time and over the course of the aging processes are presented.

With regard to the acoustic properties of hemp shiv, the acoustic absorption coefficient and transmission loss are respectively presented, in Figure 4-a and Figure 4-b for the initial batch A_0 and the batches aged with A_{Ref}, A_{HD} and A_{Ext} conditions. For A_{Ref}, the acoustic behaviour does not vary between A_0 and 24 months. The results for that environment are represented in the form of a grey curve beam for α and TL, corresponding to the extant results over two years. The α_{max} of 0.91 is obtained at a frequency of 1350 Hz. For the same frequency the value of TL is around 3 dB. With regard to A_{HD} aging process, a shift toward low frequencies is visible at 1250 Hz for the acoustic absorption curve from 3 months of aging. This value then remains stable for the rest of the aging process. The value of α_{max} also evolves over time, showing an increase at 3 months, from 0.91 to 0.93, and then a gradual decrease as aging continues, to α_{max} = 0.87. Finally, with A_{Ext}, the same shift of α_{max} (0.89) is obtained around a frequency of 1250 Hz to 1 year. Conversely, after 2 years of aging in these conditions, a significant variation of the acoustic behaviour is observed, with a sharper drop in the value of α_{max} associated with a shift of the curve towards higher frequencies. The value of 0.80 is obtained at a frequency of 1475 Hz. Thus, a reduction in transmission loss is also measured.

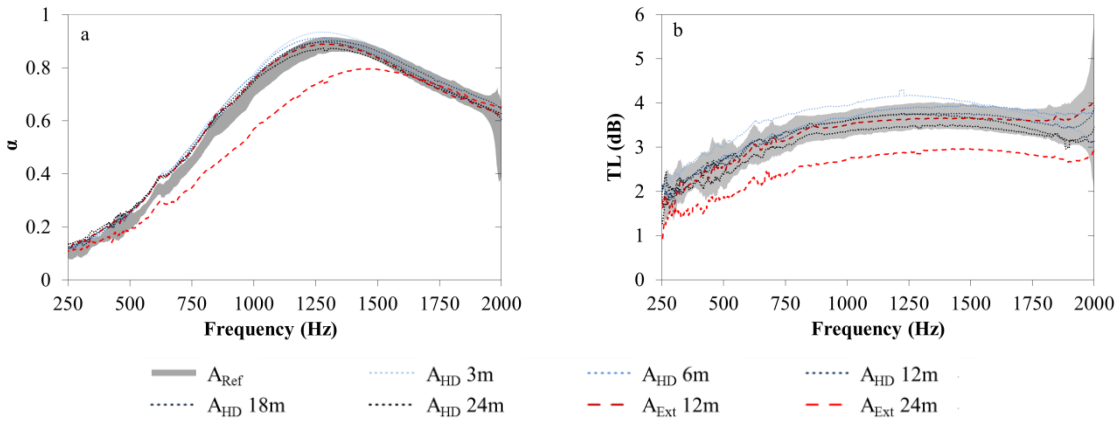

Figure 4. a) Acoustic absorption coefficient and b) transmission loss over a frequency range from 250 to 2000 Hz for hemp shiv over time and as a function of the aging processes

Another important functional property of hemp shiv is its water vapour sorption capacity. The water vapour sorption isotherms are obtained for A_0 and 18 months with A_{Ref}, A_{HD} and A_{Ext} aging processes (Figure 5). There is no discernible difference for aging A_{Ref} with A_0 between 0 and 80% RH. For A_{HD}, the water sorption increases over a range of relative humidity between 20% and 80% RH. After 18 months of aging A_{Ext}, the phenomenon is even more marked. Using the GAB model, it is possible to calculate the specific surface area for water vapour sorption (Table 2). An increase in specific surface area is observed over the course of aging A_{HD}, and also for aging A_{Ext}, though it is more marked in the latter case.

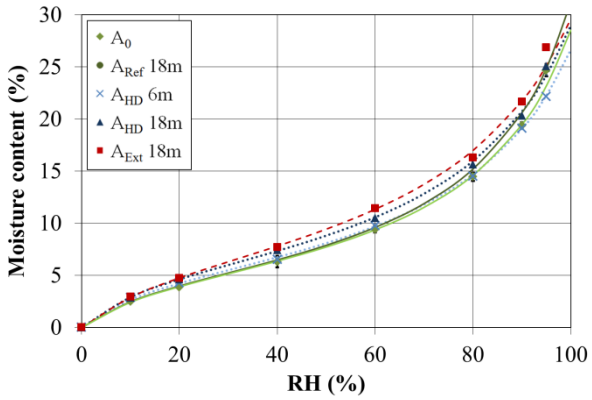

Figure 5. Sorption isotherms for hemp shiv A_0, aged for 18 months by A_{Ref}, A_{HD} and A_{Ext}, with curves generated by the GAB model.

	A_0	A_{Ref} 18m	A_{HD} 18m	A_{Ext} 18m
ω_m (%)	5.4	5.5	6.3	7.1
C	7.8	7.5	8.7	7.2
K	0.82	0.83	0.79	0.77
Specific surface area (cm²/g)	182 ± 3	186 ± 3	210 ± 5	237 ± 8

Table 2. Parameters of the GAB model corresponding to the sorption isotherms of A_0, and 18 months of A_{Ref}, A_{HD} and A_{Ext}

The changes in the shape of the sorption isotherm curves, the increase in specific surface area and the modifications of the acoustic behaviour with A_{HD} and A_{Ext} aging processes may stem from a modification to the microstructure of the material. Hence, it is necessary to study the potential evolutions of the microstructural and chemical properties of shiv on this scale.

3.2 Microstructure of the hemp shiv

a. Mass and bulk density

The variation in mass and bulk density and volume of the bulk shiv are respectively presented in Figure 6-a and b as a function of time for the A_{HD} and A_{Ext} processes. The results of A_{Ref} are not represented, because no significant variation is observed.

The batches of shiv respectively lose 25% and 35% of their initial mass after 24 months of storage in environments A_{HD} and A_{Ext}. For aging process A_{HD}, the majority of the mass loss occurs between one and three months after the beginning of this aging

Concerning the bulk density, it decreases by almost 40% after two years of aging, for both A_{HD} and A_{Ext}. Considering values obtained for A_{HD}, the drop is observed during the first three months.

From the values of bulk density and mass variations, it is possible to calculate the apparent volume variations of the particles. During the first month of aging A_{HD}, the density falls from 118 kg.m^{-3} to 90 kg.m^{-3} without a significant loss of mass. This can be explained by the swelling of the particles with an increase in apparent volume of around 30%. Between one and three months of A_{HD}, the particles mass decreases, as well as the bulk density, leading to a constant apparent volume. Then, until 24 months of A_{HD} aging, the apparent volume slightly decreases, resulting from a slow decrease of the particles mass whereas their density is constant. However, the volume of hemp shiv after two years of aging remains 16% higher than the initial one. For A_{Ext}, the apparent volume at 12 months rises by 30%, and then drops to a value 8% higher than the initial one.

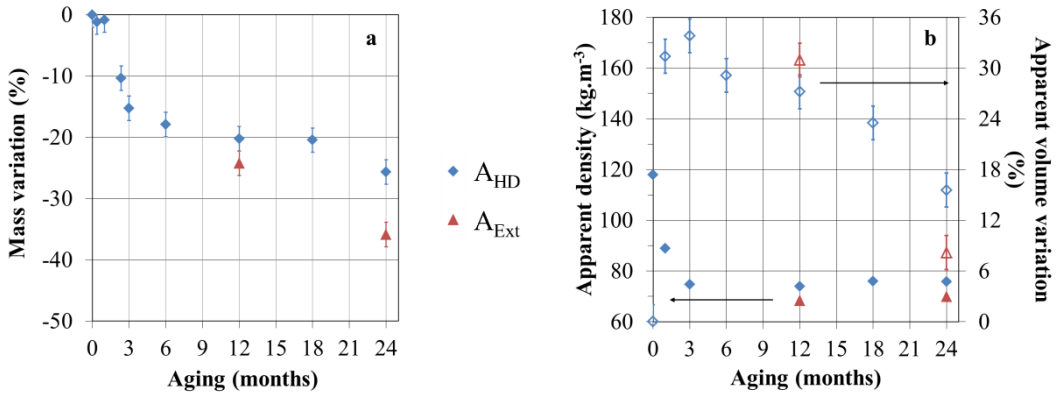

298 *Figure 6. Evolution of a batch of hemp shiv during A_{HD} and A_{Ext} aging conditions: a) mass of*
299 *shiv; b) Bulk density (full symbols) and apparent volume variation (empty symbols)*

300 *b. Density of the vegetal cell walls*

301 In order to quantify the vegetal cell wall density $\rho_{cell\ wall}$, helium pycnometer
302 measurements are performed on powdered hemp shiv (Table 3). In this case, this powder is
303 not expected to contain porosities anymore. The cell wall density value obtained is 1480 kg.m-
304 ^{3}. This value is not far off the density of the cell wall given in the existing literature for hemp
305 shiv (1450 kg.m^{-3} [32]), wood (between 1497 and 1529 kg.m^{-3} [33]) or flax and hemp fibres
306 (between 1480 and 1540 kg.m^{-3} [34] [35]). After two years of A_{HD} and A_{Ext} aging, this density
307 increases, mainly for A_{HD} conditions.

	Powdered hemp shiv A_0	**Powdered hemp shiv 2 years A_{HD}**	Powdered hemp shiv **2 years A_{Ext}**
Cell wall density (kg.m^{-3})	1480 ± 4	1531 ± 5	1498 ± 5

308 *Table 3. Skeleton density of hemp shiv determined by helium pycnometer measurements in*
309 *powder at A_0 and after 24 months in A_{HD} and A_{Ext}*

310 *c. Skeleton density*

311 The skeleton density is another parameter that can be used to characterise the
312 microstructure of bulk hemp shiv. The values of skeleton density obtained on particles with
313 an air porosimeter over time, and over the course of the different aging processes, are shown
314 in Figure 7.

315 For shiv exposed to the reference environment, a mean value over the 2 years of 872 ± 20
316 kg/m^{3} is measured. However, during six months of A_{HD} aging, the skeleton density increases
317 significantly until a constant value of 1385 ± 46 kg.m^{-3}. Values of ρ_{sk} of the same order of
318 magnitude are obtained for A_{Ext}. Comparing these values to $\rho_{cell\ wall}$, the conclusion is that a
319 portion of the porosity of the shiv is initially closed, and is therefore included in the skeleton
320 volume of the material when it is measured, leading to a low skeleton density value. As a

consequence, with aging, the increase of the skeleton density can be explained by the fact that this porosity opens and becomes accessible to air.

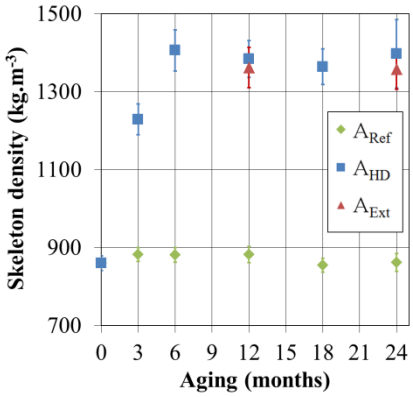

Figure 7. Skeleton density of hemp shiv by air porosimetry for hemp shiv under A_{Ref}, A_{HD} and A_{Ext} aging conditions

d. Microstructural parameters obtained from acoustic analyses

The microstructural parameters obtained from the acoustical measurements can also be used to describe the microstructure of hemp shiv (Figure 8). As with the curves for α and TL, the results for the reference environment are represented in the form of a beam of values in grey in the figures for the set of parameters. The acoustical porosity Φ_{acou} increases after 6 months for A_{HD}, and reaches a value of 0.87 at 24 months. For A_{Ext}, a similar behaviour is observed at 12 months, while the acoustical porosity tends to decrease at 24 months. The results in terms of air resistivity σ show a slight decrease in the course of both aging processes. The tortuosity α_∞ increases progressively during aging A_{HD}, reaching a value of around 2.25. On the other hand, the behaviour of this parameter is different for aging A_{Ext}, with a similar increase at 12 months, but a decrease in tortuosity is seen at 24 months. Finally, the characteristic viscous length Λ decreases at 3 months for A_{HD}, then increases again and re-joins the values of A_{Ref}. It increases after 24 months in A_{Ext}.

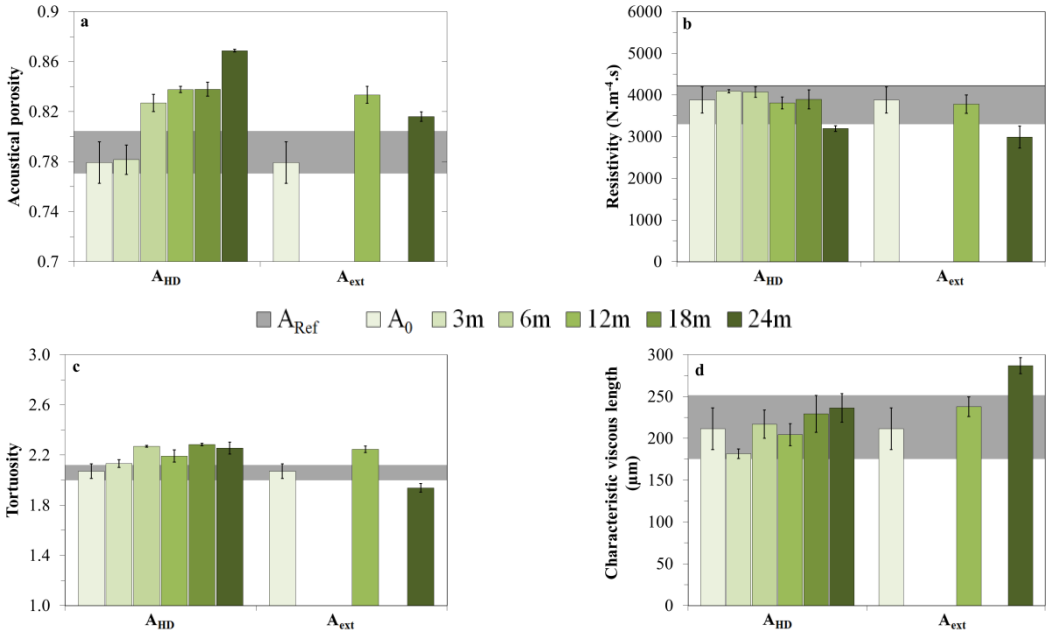

Figure 8. Variation of the acoustical parameters during aging: a) Acoustical porosity Φ_{acou}; b) tortuosity α_∞; c) resistivity σ; d) characteristic viscous length Λ for A_{Ref}, A_{HD} and A_{Ext}

e. Observation of hemp shiv during aging

In parallel with the quantification of the microstructural parameters and the description of their evolution during the different aging conditions, it is also possible to observe these modifications by scanning electron microscopy. Firstly, Figure 9 illustrates the structure of shiv before aging. In Figure 9-a, a transverse slice of a particle is visible. With greater magnification (Figure 9-b), the tracheids can be better distinguished from the vessels, as the latter are larger in diameter (≈50 µm). The longitudinal slice in Figure 9-c shows the alignment of the cells. Finally, Figure 9-d of a vessel shows the pits, the valves between the cells between 1 and 2 µm in diameter. The observation of these particles during A_{Ref} aging conditions did not show any significant evolution of plant microstructure.

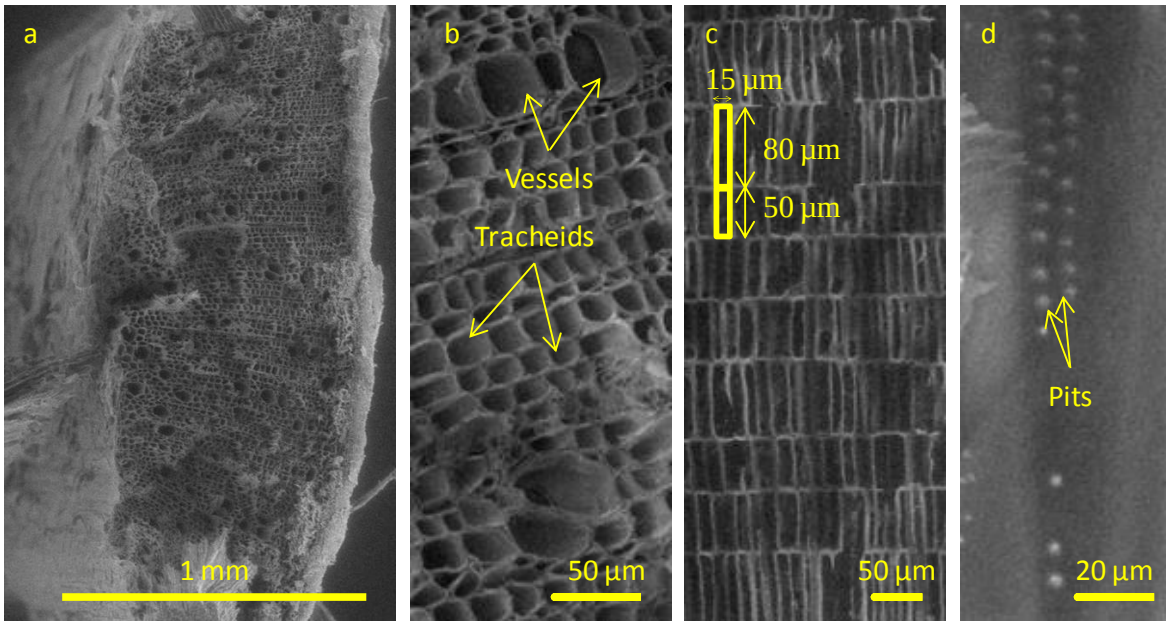

Figure 9. SEM pictures of hemp shiv before aging: a) transverse cross-section; b) transverse cross-section with tracheids and vessels; c) longitudinal cross-section; d) pits in longitudinal cross-section

The images in Figure 10 are taken on hemp shiv after 15 months of A_{HD} aging. Even though the overall structure of the particles remains unchanged (Figure 10-a), hyphae are present in large numbers on the surface of the particles (Figure 10-b). On other zones of the surface (Figure 10-c), hyphae are present, but also of perforations in the cell wall, which are not as regular as the pits visible in Figure 9-d. The analysis of transverse cross-section (Figure 10-d) shows hyphae, which are thus present within the hemp shiv, and the debonding of the cells from one another. These observations were not made after 15 months of A_{Ref} aging conditions. The perforations and the decohesion of the cellules are also observed in studies regarding the attack of fungi on wood. According to these studies, the attack on the cell wall, leading to a reduction in its thickness, affects hemicellulose and cellulose [36] [37] [38]; the decohesion of cells is due to delignification of the plant matter [39] [40] [41]. Another phenomenon is visible in Figure 10-e: a pit seems to have ripped open, leaving a hole in the cell wall over 30 µm in diameter. That tearing of the alveolus may be due to the cycles of swelling and shrinkage caused by the cycles of humidification and drying.

Overall, the same conclusions can be drawn for hemp shiv 15 months aged by A_{Ext}, with the exception of the fact that micro-organisms are present in a larger quantity (Figure 11-a) and other species of micro-organisms are found (Figure 11-b and Figure 11-c). Perforations in the cell wall are also visible, as well as hyphae and a debonding of cells.

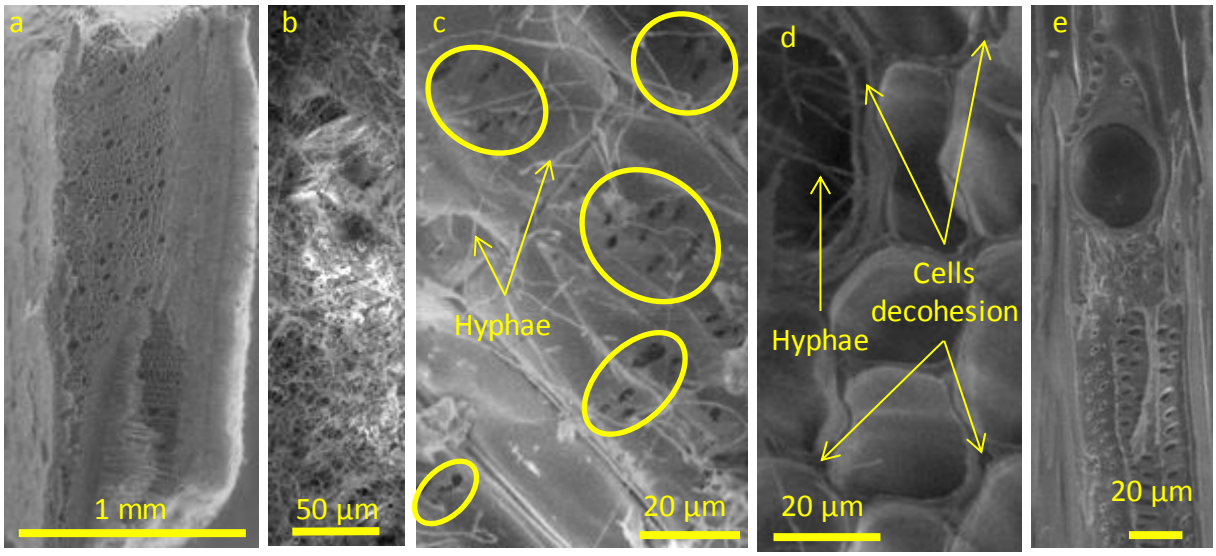

Figure 10. SEM pictures of hemp shiv after 15 months in HD aging conditions: a) transervsal cross-section; b) hyphae on the surface of a particle; c) hyphae and holes in the cell wall on the surface of a particle; d) hyphae and decohesion of cells in transversal cross-section; e) pits and torn pit in longitudinal cross-section

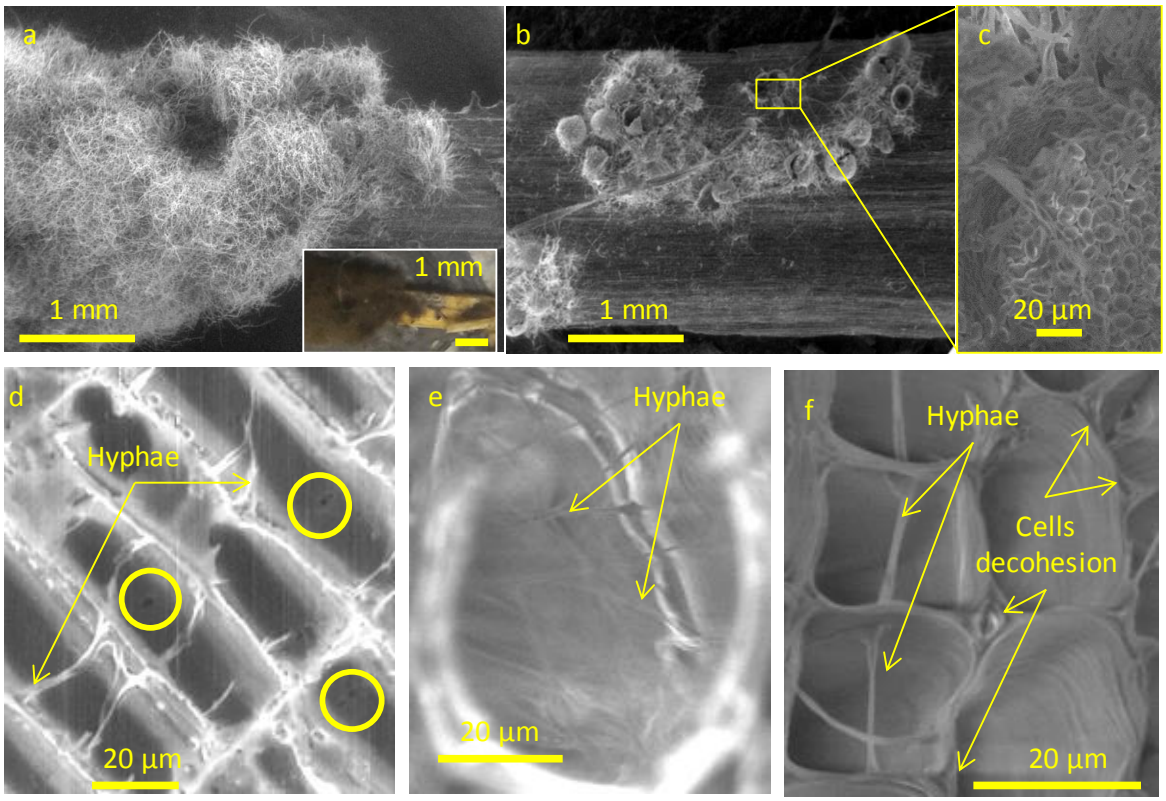

Figure 11. SEM pictures of hemp shiv after 15 months of exterior aging conditions: a) fungi on a particle with picture; b) sporiferous saccules on the surface of a particle; c) spores and hyphae inside saccule; d) hyphae and holes in cell walls viewed in longitudinal cross-section; e) hyphae in a cell in transversal cross-section; f) hyphae and decohesion of cells in transversal cross-section

3.3 Chemical composition

The chemical composition of hemp shiv for A_0, and after 24 months of A_{HD} and A_{Ext} agings conditions are presented Figure 12. The evolution of the mass fraction of cellulose, hemicelluloses and lignin of the vegetal cell walls is visible. Pectin, proteins, lipids, soluble carbohydrates like low molecular mass saccharides or soluble phenolic compounds are extracted in the first step of the Van Soest method [31]. They are labelled as "other" molecules in Figure 12. For aged hemp shiv, mass fractions are presented on the base of the initial mass before aging at A_0. The mass loss measured as a function of time, plotted in Figure 6,a is also taken into account in Figure 12.

Before aging, hemp shiv is mostly based on hollocellulose which corresponds to 65.1 % of cellulose and hemicellulose. The mass ratio lignin/hollocellulose is equal to 0.23. The other compounds represent 19.9% of the mass. This value, obtained after extraction with the neutral detergent used in the Van Soest method is higher than the amount of soluble compounds extracted in water (Table 1). After 24 months of A_{HD} aging, the amounts of cellulose and lignin decrease, whereas the hemicellulose mass fraction is stable. The ratio lignin/hollocellulose decreases to 0.20, lower than for A_0. The quantity of other compounds is also lower than for A_0. Finally after two years of exterior aging, a large decrease of the cellulose, hemicellulose and lignin amounts is observed. The total quantity of these three hemp shiv components represents 27 % of the total mass of shiv, whereas they represent more than 80% of the initial mass. Moreover, the amount of other molecules is higher than before aging.

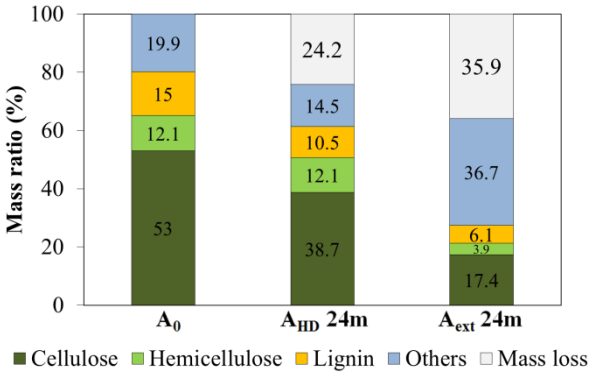

Figure 12. Chemical composition of hemp shiv (cellulose, hemicelluloses and lignin) at A_0, and after 24 months in A_{HD} and A_{Ext} aging conditions

4 Discussion

The results presented show some differences in the variations of the functional properties as a function of the environment applied to hemp shiv. For the reference conditions A_{Ref}, no significant variation is observed; the shiv retains all of its properties over time. As regards A_{HD} aging, variations in the acoustic and hydric behaviour are visible. This aging induces a shift toward low frequencies in the curve of α with variations of α_{max} over time, and an increase in

water vapour sorption capacity (Figure 4-a and Figure 5). With the A_{Ext} aging process, the modifications in the functional properties are more marked. Indeed, a shift in the acoustic absorption curve toward higher frequencies is noted, with a significant drop in the maximum value reached (Figure 4), a reduction in the transmission loss and an increase in water vapour sorption capacity that is even greater than for A_{HD} conditions (Figure 5).

In order to understand the aging mechanisms causing the modifications in functional properties, the microstructure has been studied using different complementary characterisation methods. Three major modifications of properties due to A_{HD} and A_{Ext} agings, and an additional phenomenon for A_{Ext} are observed:

- a loss of mass;
- variations in volume with swelling followed by shrinkage;
- an opening of the porosity that was initially closed;
- an increase in the distribution of pore sizes for A_{Ext}.

An illustration of the evolution of the microstructure in the material over time for the different aging conditions is given in Figure 13. The different volume fractions of a batch of hemp shiv are represented by using the values of the volume fractions of the vegetal cell wall $\eta_{cell\ wall}$, closed intraparticle porosity Φ_{intra_closed}, opened intraparticle porosity Φ_{intra_opened}, interparticle porosity Φ_{inter} and acoustic porosity Φ_{acou}. The four aging phenomena identified are visible in the illustration reported on Figure 13 and are described one by one in the next paragraphs.

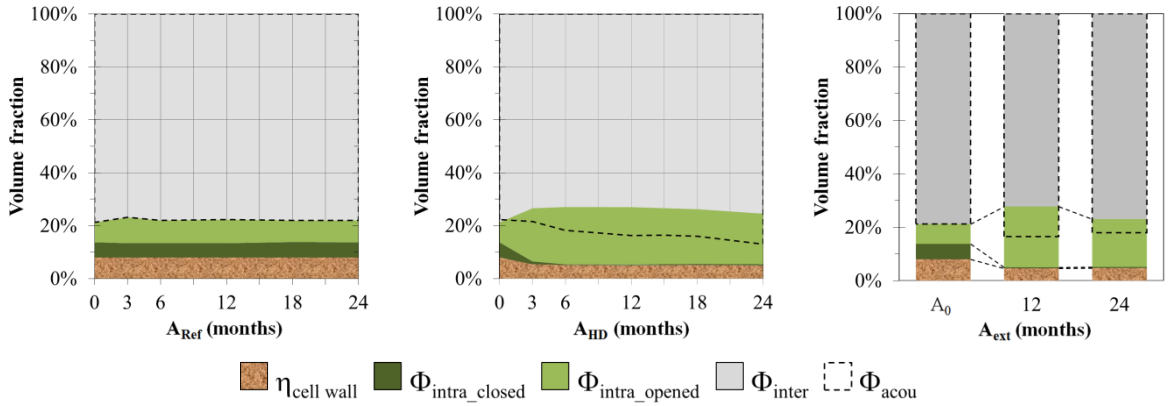

Figure 13. Volume fraction of hemp shiv in bulk for: a) reference conditions; b) HD aging; c) Ext aging

The first phenomenon is a mass loss of 25% for 24 months in A_{HD} and 35% for 24 months in A_{Ext} conditions (Figure 6-a). The rate of extractible molecules initially contained in the particles, which is about 20 % (Figure 11) cannot fully explain the mass loss values obtained. Thus, the structure of the plant matter is also altered during aging by the attack of micro-organisms, as observed by SEM in Figure 10 and Figure 11. A targeted degradation according to the type of aging process can be deduced from the density values of the cell wall measured

with a helium pycnometer (Table 3). Indeed, cellulose, hemicellulose and lignin respectively have a density of 1559 $kg.m^{-3}$, 1520 $kg.m^{-3}$ and 1260 $kg.m^{-3}$ [42]. As the ratio lignin/hollocellulose after aging is found lower than before aging (Figure 12), the greatest increase in $\rho_{cell\ wall}$ after A_{HD} aging may indicates a preferential attack on the lignin. Due to a higher proportion of hollocellulose, the cell wall density increases. Moreover, cells decohesion observed in Figure 10-d, which is the consequence of an attack on lignin, confirms this explanations. For A_{Ext}, the structure of hemp shiv is more severely damaged with less than 30 % of hollocellulose and lignin remaining. This severe attack on the structure is also visible during the preparation of hemp shiv for SEM observations. Indeed, most of hemp shiv is too soft to be sliced, making observations on the structure impossible. Pictures on Figure 11 show hemp particles having still enough stiffness to be cut. The impact of the mass loss on the functional properties is primarily visible after 24 months of A_{Ext} aging conditions, as it is directly responsible for the decrease in transmission loss (Figure 4-b).

The second modification identified is the succession of two steps, regarding the volume variation of the batches of shiv in A_{HD} and A_{Ext} aging conditions, namely swelling followed by shrinkage of batches of hemp shiv up to 24 months. The swelling is visible thanks to the evolutions of the bulk density and of the mass loss measured (Figure 6-a and b). In the volume set for the acoustic measurements, the swelling of the particles leads to a decrease of the interparticle porosity, as it is necessary to further compact the particles which are placed in a constant volume. However, in the diagram of figure 13, the acoustical porosity increases. Thus, it is no longer possible to make the assumption that Φ_{acou} corresponds to Φ_{inter}. This point is discussed in the next paragraph. The swelling is therefore represented on the basis of the increase in apparent volume. The effect of the swelling is also visible with the increase in air resistivity σ and the decrease of the viscous characteristic length Λ (Figure 8-b and d). Indeed, with the lowering of the interparticle porosity, it becomes more difficult for air to pass through the material, with a smaller noticeable pore size in acoustic terms. The shrinkage of the bulk hemp shiv is observed after 3 months with a stabilisation of the bulk density associated to the mass loss (Figure 6-a and b). Here, once again, the acoustic parameters are affected. With shrinkage, σ progressively decreases and Λ recovers (Figure 8-b and d). For the A_{HD} aging process, the swelling of particles increases from a value of +35 % at 3 months to +18 % at 24 months, with respect to the initial volume. The volume variation for A_{Ext} even drops to 8% in relation to the initial volume after 24 months of aging. In terms of functional properties, these variations in resistivity account for the increase in α_{max} for the acoustic absorption curve after 3 months, and then the gradual decrease of this value as aging A_{HD} progresses (Figure 4-a and Figure 8-b). These swellings can be explained by water absorption, which causes a deformation of the particles, no longer holds true without a recovering of their initial size after drying. Over the course of aging and the mass loss of the material, the structure of the plant is sufficiently deteriorated by the micro-organisms to cause the particles to shrink over time (Figure 10 and Figure 11).

The next phenomenon is the opening of the porosity in the hemp shiv, which, initially, is partly closed or inaccessible for measurement, whether with air or acoustic waves. Indeed, the increase of the skeleton density and its stabilisation over time after 6 months show that a part of the porosity is not initially accessible to the air (Figure 7). The opened porosity at A_0 is 86.3 %, when the total porosity is estimated at 92.0 %. This opening of the porosity Φ_{intra_closed} is visible in Figure 11. Two types of actions lead to this opening of the porosity. The first one is the attack of the cell wall by micro-organisms, which can be seen by the perforations in the structure of the hemp shiv (Figure 9 and Figure 11). The second one is the action of water, with the swelling of the particles leading to the expansion of the pores and the tearing of the pits after cell wall deformation (Figure 10-e). After aging, the originally closed porosity is practically totally open, the values of the open air porosity and total porosity being respectively 94.6 % and 95.0 % after A_{HD} aging, and 94.9% and 95.3 % for A_{Ext} aging. In addition of the opening of the initially closed porosity, there is an increase of the total porosity explained by the loss of matter after the various aging processes. A portion of the porosity also becomes accessible to sound waves. Indeed, the tortuosity increases, as does the acoustic porosity, visible in the diagram (Figure 8-a and c). This means that the hypothesis put forward for A_0, whereby only the interparticle porosity plays a role in acoustics, no longer holds true. The acoustic wave is then also dissipated by a portion of the intraparticle porosity. The contrast between the two types of porosity remains significant – a multi-porous system is obtained. This phenomenon is observed for A_{HD} aging up to 24 months and A_{Ext} at 12 months. The impact of this opening of porosity on the functional properties is an increase of the water vapour sorption capacity, associated with an increase of the specific surface area S_m determined by sorption measurements (Figure 5). The increase in tortuosity is responsible for the shift toward lower frequencies in the acoustic absorption curve (Figure 4-a).

A final modification of structure must be added to the opening of the porosity to explain the behaviour of hemp shiv at 24 months of A_{Ext} aging. In this case, the tortuosity increases at 12 months, and then decreases, eventually reaching a value lower than the initial one (Figure 8-c). The acoustic porosity also decreases, whereas the characteristic viscous length increases (Figure 8-a and d). In this case, the openings of pores after the degradation of the hemp shiv are sufficiently significant so that there is no longer a contrast between the interparticle porosity and intraparticle porosity acoustically accessible, a single-porosity system is obtained once again. The path of the acoustic wave is therefore shorter, the tortuosity decreases sharply, and the size of the viscous characteristic length increases. This decrease in tortuosity and the increase of Λ are responsible for the shift towards higher frequencies and for the sharp decrease in the maximum of the acoustic absorption curve (Figure 4-a).

5 CONCLUSION

In this article, different characteristic modifications due to aging of hemp shiv were highlighted. Three different environments have been applied to bulk hemp shiv during two

519 years: reference conditions (A_{Ref}) at 50% RH, hygric aging with variations in relative humidity
520 at 30°C (A_{HD}) and an outdoor aging process corresponding to real weather conditions (A_{Ext}).

521 For the reference conditions A_{Ref}, no significant variation in the functional or microstructural
522 properties was observed. In these hygrothermic conditions which exist in a building, the
523 properties of shiv do not vary over time, so the durability of the material over time is good.

524 For the A_{HD} accelerated aging process, which applies an average humidity of over 80%, with
525 the majority of time spent at 98% RH, three phenomena are part of aging mechanism,
526 inducing evolution of the microstructure and of the functional properties of hemp shiv are
527 observed:

528 - a mass loss, which can go so far as to decrease the material's properties in terms of
529 acoustic insulation;
530 - volume variations which play a part in acoustic absorption;
531 - an opening of the porosity, leading to a higher water vapour sorption capacity, and a
532 change in the acoustic absorption.

533 Finally, for A_{Ext} aging, a fourth phenomenon is added to the first three: the modification of the
534 pore size distribution, which has a significant impact on the sound absorption.
535 The role of micro-organisms as mechanism of the phenomena is demonstrated. Fungal attack
536 alters the microstructure of the hemp shiv, and therefore its functional properties. The micro-
537 organisms develop for the accelerated aging A_{HD}, but not for aging A_{Ref}.

538 The accelerated aging, then, modifies the properties of the hemp shiv, but needs to be
539 compared to conditions of aging in a real-world building in order to be able to estimate the
540 lifetime of the bulk hemp shiv whilst guaranteeing it will retain its functional properties. In
541 the case of hemp-based concrete, it is therefore necessary to monitor fungal development in
542 the material over time, and also any modifications in porosity, which may be indicative of
543 fungal development within the hemp concrete. Moreover, in hemp concrete the aggregates are
544 protected by an alkaline binder. It could be interesting to study if the same aging mechanisms
545 are obtained.

546 ## Funding

547 The DVS measurements were supported by public funds received in the framework of SENSE-
548 CITY, a project (ANR-10-EQPX-20) of the program 'Investissements d'Avenir' managed by the
549 French National Research Agency.

550 ## Data availability

551 The raw/processed data required to reproduce these findings cannot be shared at this time as
552 the data also forms part of an ongoing study.

553 **6 REFERENCES**

[1] S. Amziane and L. Arnaud, Les bétons de granulats d'origine végétale. Application au béton de chanvre, Lavoisier, 2013.

[2] G. Delannoy, S. Marceau, P. Glé, E. Gourlay, M. Guéguen-Minerbe, D. Diafi, I. Nour, S. Amziane and F. Farcas, "Influence of binder on the multiscale analysis of hemp concretes" *European Journal of Environmental and Civil Engineering,* 2018, DOI: 10.1080/19648189.2018.1457571.

[3] R. Walker, S. Pavia and R. Mitchell, "Mechanical properties and durability of hemp-lime concretes" *Construction and Buildings Materials,* vol. 61, pp. 340-348, 2014.

[4] Sassoni, E. Sassoni, S. Manzi, A. Motori, M. Montecchi and M. Canti, "Experimental study on the physical-mechanical durability of innovative hemp-based composites for the building industry" *Energy and Buildings,* vol. 104, pp. 316-322, 2015.

[5] S. Marceau and G. Delannoy, "Durability of Bio-based concretes" in *Bio-aggregates Based Building Materials, RILEM State-of-the-Art reports*, vol. 23, S. Amziane and F. Collet, Eds., Dordrecht, Springer, 2017, pp. 167-187.

[6] S. Marceau, P. Glé, M. Guéguen-Minerbe, E. Gourlay, S. Moscardelli, I. Nour and S. Amziane, "Influence of accelerated aging on the properties of hemp concretes" *Construction and Building Materials,* vol. 139, pp. 524-530, 2017.

[7] A. Arizzi, H. Viles, I. Martin-Sanchez and G. Cultrone, "Predicting the long-term durability of hemp-lime renders in island and coastal areas using Mediterranean, Tropical and Semi-arid climatic simulations" *Science of Total Environment,* vol. 542, pp. 757-770, 2016.

[8] M. Kutnik, E. Suttie and C. Brischke, "Durability, efficacity and performance of bio-based construction materials: Standardisation background and systems of evaluation and authorisation for the European market" in *Performance of Bio-Based Building Materials*, Woodhead publishing, 2017, pp. 593-610.

[9] Y. Xia, T. Chen, J. Wen, Y. Zhao, J. Qiu and R. Sun, "Multi-analysis of chemical transformations of lignin macromolecules from waterlogged archaeological wood" *International Journal of Biological Macromolecules,* vol. 109, pp. 407-416, 2018.

[10] M. Riggio, J. Sandak, A. Sandak, D. Pauliny and L. Babinski, "Analysis and prediction of selected mechanical/dynamic properties of wood after short and long-term waterlogging" *Construction and Building Materials,* vol. 68, pp. 444-454, 2014.

[11] P. Evans and W. Banks, "Degradation of wood surfaces by water" *Holz als Roh- und Werkstoff,* vol. 48, pp. 159-163, 1990.

[12] S. Graham, I. Ogunfayo, M. Hall, C. Snape, W. Quick, S. Weatherstone and C. Eastwick, "Changes in mechanical properties of wood pellets during artifical degradation in a laboratory environment" *Fuel Processing Technology,* vol. 148, pp. 395-402, 2016.

[13] S. Graham, C. Eastwick, C. Snape and W. Quick, "Mechanical degradation of biomass wood pellets during long term stockpile storage" *Fuel Processing Technology,* vol. 160, pp. 143-

151, 2017.

[14] C. Popescu and M. Popescu, "A near infrared spectroscopic study on the structural modifications of lime (Tilia cordata Mill.) wood during hydro-thermal treatment" *Spectrochimia acta Part A: molecular and biomolecular spectroscopy,* vol. 115, pp. 227-233, 2013.

[15] A. Cogulet, P. Blanchet, V. Landry and P. Morris, "Weathering of wood coated with semi-clear coating: Study of interactions between photo and biodegradation" *International Biodeterioration & Biodegradation,* vol. 129, pp. 33-41, 2018.

[16] C. Brischke, L. Meyer-Veltrup and T. Bornemann, "Moisture performance and durability of wooden facades and decking during six years of outdoor exposure" *Jounral of Building Engineering,* vol. 13, pp. 207-215, 2017.

[17] C. Brischke and S. Thelandersson, "Modelling the outdoor performance of wood products - A review on existing approaches" *Construction and Building Materials,* vol. 66, pp. 384-397, 2014.

[18] T. Noguchi, E. Obataya and K. Ando, "Effects of aging on the vibrational properties of wood" *Journal of Cultural Heritage,* vol. 13S, pp. S21-S25, 2012.

[19] W. Sondergger, K. Kranitz, C. Bues and P. Niemz, "Aging effects on physical and mechanical properties of spruce, fir and oak wood" *Journal of Cultural Heritage,* vol. 16, no. 6, pp. 883-889, 2015.

[20] E. Obataya, "Effect of natural and artifical ageing on the physical and acoustical properties of wood in musical instruments" *Journal of Cultural Heritage,* vol. 27, pp. 63-69, 2017.

[21] B. Pejic, M. Kostic, P. Skundric and J. Praskalo, "The effects of hemicelluloses and lignin removal on water uptake behavior of hemp fibers" *Bioressource technology,* vol. 99, pp. 7152-7159, 2008.

[22] N. Dujardin, V. Feuillet, D. Garon, L. Ibos, M. Marchetti, L. Peiffer, D. Pottier, V. Séguin and D. Theile, "Impacts of environmental exposure on thermal and mycological characteristics of insulation wools" *Environmental Impact Assessment Review,* vol. 68, pp. 66-80, 2018.

[23] M. Liu, D. Fernando, G. Daniel, Madsen B., A. Meyer, M. Ale and A. Thygesen, "Effect of harvest time and field retting duration on the chemical composition, morphology and mechanical properties of hemp fibers" *Industrial Crops and Products,* vol. 69, pp. 25-39, 2015.

[24] I. Le Bayon, M. Draghi, M. Gabille, M. Prégnac and et al., "Development of a laboratory test method to assess the resistance of bio-based insulation materials against moulds" in *1st ICBBM*, Clermont-Ferrand, 2015.

[25] B. Stefanowski, S. Curling and G. Ormondroyd, "A rapid screening method to determine susceptibility of bio-based construction and insulation products to mouls growth"

International Biodeterioration & Biodegradation, vol. 116, pp. 124-132, 2017.

[26] S. Amziane, F. Collet, M. Lawrence, C. Magniont, V. Picandet and M. Sonebi, "Recommandation of the RILEM TC 236-BBM: characterization testing of hemp shiv to determine the inital water content, water absorption, dry density, particle size distribution and thermal conductivity" *Materials and Structures,* vol. 50:167, 2017.

[27] P. Glé, E. Gourdon and L. Arnaud, "Modelling of acoustical properties of hemp particles" *Construction and Building Materials,* vol. 37, pp. 801-811, 2012.

[28] Y. Jiang, M. Lawrence, M. Ansell and A. Hussain, "Cell wall microstructure, pore size distribution and absolute density of hemp shiv" *Royal Society Open Science,* vol. 5, pp. 1-15, 2018.

[29] E. Gourlay, P. Glé, S. Marceau, C. Foy and S. Moscardelli, "Effet of water content on the acoustical and thermal properties of hemp concretes" *Construction and Building Materials,* vol. 139, pp. 513-523, 2017.

[30] C. Zwikker and C. Kosten, Sound absorbing Materials, New York: Elsevier, 1949.

[31] AFNOR, "NF V18-122 - Aliments des animaux - Détermination séquentielle des constituants pariétaux - Méthode par traitement aux détergents neutre et acide et à l'acide sulfurique" 2013.

[32] V. Picandet, "Bulk density and Compressibility" in *Bio-aggregates Based Building Materials, RILEM State-of-the-Art reports, 23*, A. S. a. C. F., Ed., Dordrecht, Springer, 2017, pp. 167-187.

[33] R. Kellog and F. Wangaard, "Variation in the cell-wall density of wood" *Wood and Fiber Science,* vol. 3, pp. 180-204, 1969.

[34] C. Baley, "Fibres naturelles de renfort pour matériaux composites" Techniques de l'Ingénieur, 2005.

[35] C. Garcia-Jaldon, D. Dupeyre and M. Vignon, "Fibres from semi-retted bundles by steam explosion treatment" *Biomass & Bioenergy,* vol. 14, pp. 251-260, 1998.

[36] C. Hills and A. Papadopoulos, "A review of methods used to determine the size of cell wall microvoids of wood" *Journal of Institue of wood science,* vol. 15, pp. 337-345, 2001.

[37] F. Green, T. Tschernitz, T. Kuster and T. Highley, "Hydrolysis of bordered pits during colonization of wood by brown-rot fungi" Internation Research group on wood preservation, 1995.

[38] F. Schwarze, G. DeFloroio and S. Fink, "Resistance of parenchyma cells in wood to degradation by brown rot fungi" *Mycological Progress,* vol. 2, pp. 267-274, 2003.

[39] F. Schwarze, "Wood decay under the microscope" *Fungal Biology Reviews,* vol. 21, pp. 133-170, 2007.

[40] R. Peek, W. Liese and N. Parameswaran, "Infektion und Abbau des Wurzelholzes von Fichten durch Fomes annosus" *European Journal of Forest Pathology,* vol. 2, pp. 237-248, 1972.

[41] R. Blanchette, “Selective delignification of eastern hemlock by Ganoderma tsugae” *Phytopathology,* vol. 74, pp. 153-160, 1984.

[42] Y. Chen, Q. Yu and H. Brouwers, “Acoustic performance and microstructural analysis of bio-based lightweight concrete containing miscanthus” *Construction and Building Materials,* vol. 157, pp. 839-851, 2017.

554

555